Original Article

Role of STK38L in atrial fibrillation-associated myocardial fibrosis: findings from RNA-seq analysis

Yu Zhang[1,2]^, Ru Zhang[2], Xiaochen Wang[2], Sihua Fang[2], Bangning Wang[1]

[1]Department of Cardiology, The First Affiliated Hospital of Anhui Medical University, Hefei, China; [2]Department of Cardiology, The Second Affiliated Hospital of Anhui Medical University, Hefei, China

Contributions: (I) Conception and design: Y Zhang; (II) Administrative support: B Wang; (III) Provision of study materials or patients: R Zhang, S Fang; (IV) Collection and assembly of data: Y Zhang; (V) Analysis and interpretation of data: Y Zhang, X Wang; (VI) Manuscript writing: All authors; (VII) Final approval of manuscript: All authors.

Correspondence to: Yu Zhang, MD. Department of Cardiology, The First Affiliated Hospital of Anhui Medical University, No. 120 Wanshui Road, Hefei 230022, China; Department of Cardiology, The Second Affiliated Hospital of Anhui Medical University, Hefei, China. Email: zhangyu@ahmu.edu.cn; Bangning Wang, MD. Department of Cardiology, The First Affiliated Hospital of Anhui Medical University, No. 120 Wanshui Road, Hefei 230022, China. Email: wangbangning@medmail.com.cn.

Background: Myocardial fibrosis is a key pathological feature of many cardiovascular diseases, leading to cardiac dysfunction. Transforming growth factor β1 (TGF-β1) induces the proliferation and activation of cardiac fibroblasts (CFs), key contributors to myocardial fibrosis. To explore the mechanism underlying myocardial fibrosis, we aimed to determine whether serine/threonine kinase 38 like (STK38L) contributes to the development of myocardial fibrosis by regulating the proliferation and activation of CFs triggered by TGF-β1.

Methods: In this study, atrial tissue samples from atrial fibrillation (AF) patients with features of myocardial fibrosis (a category of atrial cardiomyopathy) and sinus rhythm (SR) patients without myocardial fibrosis were collected for RNA sequencing (RNA-seq). The specific molecule STK38L was identified. Primary mouse CFs were activated with TGF-β1 and subsequently transfected with STK38L-small interfering RNA (siRNA). The effect of STK38L-siRNA on fibroblast activation and proliferation was assessed using scratch and Cell Counting Kit-8 (CCK-8) assays. Furthermore, a mouse model of myocardial fibrosis induced by continuous subcutaneous injection of isoprenaline (ISO) was established to assess *STK38L* expression levels. Molecular experiments confirmed the expression of STK38L in fibrotic atrial tissues, ventricular tissues of ISO mouse, and primary CFs of neonatal mice

Results: We identified 1,870 genes exhibiting differential expression in the RNA-seq data between the AF and SR groups. Masson's trichrome staining revealed increased fibrosis in the heart tissues of the AF group. Elevated levels of STK38L were observed in the atrial tissues of the AF group and in the TGF-β1-stimulated primary mouse CFs. *In vitro*, STK38L knockdown suppressed mouse CFs activation and proliferation. Additionally, *in vivo* experiments showed that elevated mRNA levels of *STK38L*, periostin (*POSTN*), and collagen type I alpha 1 chain (*COL1A1*) in ISO-treated mouse hearts correlated with greater myocardial fibrosis, suggesting that STK38L plays an important role in the development of fibrosis.

Conclusions: This study revealed a significant correlation between increased STK38L expression and AF characterized by atrial fibrosis as well as between STK38L expression and the TGF-β1-related induction of myocardial fibrosis. Additionally, STK38L knockdown was shown to suppress CFs activation and proliferation under TGF-β1 stimulation. These findings suggest an important role of STK38L in the development of fibrosis, and help screen for new strategies to treat this complex disease.

^ ORCID: 0009-0004-8885-0583.

Keywords: Atrial fibrillation (AF); atrial cardiomyopathy (ACM); serine/threonine kinase 38 like (STK38L); myocardial fibrosis

Submitted Apr 16, 2024. Accepted for publication Aug 26, 2024. Published online Oct 22, 2024.
doi: 10.21037/cdt-24-164
View this article at: https://dx.doi.org/10.21037/cdt-24-164

Introduction

Myocardial fibrosis is an important causative mechanism of several cardiac diseases and is characterized primarily by abnormal deposition of noncontractile extracellular matrix (ECM) within the myocardium (1). This process leads to structural and electrical remodeling of cardiac tissue (2). In the human heart, the atrial ECM accounts for 49% of the total volume, whereas the ventricular ECM accounts for only 17%. In contrast, the atria are more prone to fibrosis than ventricular tissue, and thus deserve to be studied in depth (3). To date, the diseases associated with atrial fibrosis are mostly grouped in the category of atrial cardiomyopathy (ACM) (4,5). ACM refers to subclinical and/or clinical electromechanical changes in the atria that underlie atrial dysfunction and create a conducive environment for the development of clinically evident atrial fibrillation (AF) (6). The clinical manifestations are mostly AF and thrombosis, which are closely related to cardiac diseases and unexplained strokes (7). These factors have a major impact on the health and survival of patients.

In this study, atrial tissues from patients with AF with substantial atrial fibrosis and from patients with sinus rhythm (SR) without fibrosis were collected for RNA sequencing (RNA-seq) analysis, Venn diagram analysis revealed that serine/threonine kinase 38 like (*STK38L*) was significantly overexpressed in the atrial tissues of patients with AF and in transforming growth factor β1 (TGF-β1)-stimulated activated human cardiac fibroblasts (CFs), and both groups of models exhibited myocardial fibrotic features (increased Masson staining and Collagen-I secretion), suggesting that STK38L may be positively correlated with atrial fibrosis. STK38L, also known as nuclear Dbf2-associated kinase 2 (NDR2), is an important serine/cellulose molecule in the NDR family, and is an important serine/threonine protein kinase that is mainly localized in the cytoplasm, cytoskeleton, and nucleus. Published studies on STK38L gene function have focused on tumor growth and migration (8), regulation of the cell cycle and cell death (9), and maintenance of innate immunity (10). STK38L and its counterpart STK38 act as YAP kinases downstream of MOB1 and MST1/2 in the Hippo pathway and therefore play important roles in organ development and homeostasis, especially neuronal development (11,12). According to the NCBI database (https://www.ncbi.nlm.nih.gov/gene/23012), *STK38L* mRNA is generally enriched in tissues such as appendages, gallbladder and heart. In addition, gene enrichment gradually increased with cardiac development (Figures S1,S2). Previously, STK38L and STK38 were knocked down in a mouse model, which resulted in a poorly developed cardiac ring and severe cardiac insufficiency, leading to death from day 8.5 in embryonic mice (13). Therefore, STK38L may be important in cardiac development, but there are few in-depth studies on this topic.

Using bioinformatics and basic experiments, we demonstrated that STK38L is closely related to multiple dimensions of myocardial fibrosis *in vivo* in human and animal cells *in vitro*. Downregulation of STK38L expression reversed TGF-β1-stimulated CFs activation and inhibited the proliferation and migration of CFs, which may be an important mechanism for inhibiting myocardial fibrosis. STK38L, as a potential new target for the treatment of

Highlight box

Key findings

- This study found that serine/threonine kinase 38 like (STK38L) promotes cardiac fibroblast proliferation and activation, which is closely associated with atrial fibrillation and transforming growth factor β1 (TGF-β1)-associated myocardial fibrosis.

What is known and what is new?

- STK38L is enriched in cardiac left ventricular tissue.
- In TGF-β1-induced myocardial fibrosis, STK38L promotes the proliferation and activation of fibroblasts.

What is the implication, and what should change now?

- STK38L may be a potential therapeutic target for myocardial fibrosis in fibrosis-related diseases, such as atrial cardiomyopathy. However, the molecular mechanisms between STK38L and its upstream and downstream factors remain to be investigated.

myocardial fibrosis, may have applications in the treatment of myocardial fibrosis-associated ACM or other heart diseases. We present this article in accordance with the ARRIVE reporting checklist (available at https://cdt.amegroups.com/article/view/10.21037/cdt-24-164/rc).

Methods

The detailed materials and methods used are described in the Appendix 1 and Tables S1-S4.

Human samples

The study was conducted in accordance with the Declaration of Helsinki (as revised in 2013). We recruited 13 patients who underwent heart valve replacement or repair and who exhibited either AF or SR. The study was approved by the ethics committee of The Second Affiliated Hospital of Anhui Medical University (No. YX2022-099). Before surgery, all participants were thoroughly informed about the research and provided their signed informed consent. The methodology employed for specimen collection and the characterization of the patients' clinical data are detailed in Table S1.

Animal models

All experiments involving animals in this study received approval from the Institutional Animal Care and Use Committee at Anhui Medical University (No. 20170296), in compliance with institutional guidelines for the care and use of animals. A protocol was prepared prior to the study but was not registered. Wild-type (WT) C57BL adult male mice (8 weeks) were purchased and bred from the Animal Experiment Center of Anhui Medical University. Twenty mice were randomly divided into a control group and an experimental group. The mice in the isoprenaline (ISO)-treated group and the vehicle control group were subjected to 14 consecutive days of subcutaneous injections of ISO (15627, Sigma, Shanghai, China) (5 mg/kg/d) and an equivalent amount of saline (0.9% NaCl, CR Double-Crane, Beijing, China) once a day for 21 consecutive days, and mouse ventricular tissues were collected for Masson's trichrome staining (14).

Cell models

- *In vitro* cell experiments (Figure S3): primary fibroblasts were successfully extracted from neonatal C57BL mammary mouse heart tissues in short (details are provided in the *Methods* section of Appendix 1). The cells were initially considered as generation 0 (G0) cells and were cultured in a 37 ℃ incubator with 5% CO_2 and 95% air for 2–3 days until they reached confluency. First to second generation CFs were subsequently selected for experiments. After the cells had adhered to the wall, they were first starved in medium containing 2% fetal bovine serum (FBS; 10091148, Gibco, Auckland, New Zealand) + 1% 100× penicillin (PEN)/Strep (15140122, Gibco) + DMEM/F12k (11320033, Gibco) for 12 h. Then, the medium was changed to 10% FBS, and 1× PEN Strep + DMEM/F12k + 10 ng/mL TGF-β1 (CK33, Novoprotein, Suzhou, China) was added to the cells in the experimental group. Afterward, the CFs were treated with the medium for 24 h to induce activation (15).
- *In vitro* cellular experiments (Figure S4): extracted mouse CFs were plated and stimulated with 10 ng/mL TGF-β1 (CK33, Novoprotein) for 24 h, and when the density was approximately 60–70%, Polyplus jetPRIME transfection kit (101000015, Polyplus, Illkirch, France) was used to transfect the STK38L-small interfering RNA (siRNA) cells to generate the STK38L knockdown cell model (16). The medium was changed for culture at 24 h. Gene function and expression levels were determined 48–72 h after transfection.

RNA-seq and differentially expressed genes (DEGs) analysis

Freshly obtained human atrial tissue was promptly submerged in RNA tissue preservation solution (G3019-100ML, Servicebio, Wuhan, China) and refrigerated at 4 ℃ for 24 h. After the preservation solution was discarded, the samples were stored in a liquid nitrogen tank for preservation and collected at the end of the collection. Then, tissue mRNA was extracted, and a sequencing library was constructed and uploaded to the high-throughput sequencing platform for sequencing (sequencing services provided by Shanghai Berhoff Biotechnology Co., Shanghai, China). Atrial tissues from 13 patients were collected for analysis in this study. Eight patients exhibited AF, while the remaining 5 exhibited SR. All sequencing samples were quality controlled. DEG analysis was performed based on COUNT data using the Bioconductor software package edgeR. Genes were considered significantly differentially

expressed if the $\log_2$ (fold change) was >1 or <−1 and the P value was less than 0.05. RNA-seq of human AF tissues revealed a total of 1,870 DEGs, 459 of which were upregulated and 1,411 of which were downregulated. The RNA-seq data from the GEO dataset GSE225336 revealed a total of 2,692 DEGs, 593 of which were upregulated and 2,099 of which were downregulated. The DEGs were visualized with heatmaps for expression distribution.

Data analysis of Gene Expression Omnibus (GEO) datasets

The RNA-seq datasets GSE225336, GSE82294, GSE97358, and GSE132143 and the single-cell transcriptome dataset GSE120064 were downloaded from the GEO database (https://www.ncbi.nlm.nih.gov/geo/) (Table S4). Specific methods for analyzing single-cell RNA-seq data and gene set enrichment analyses (GSEAs) have been added to the online supplement.

Statistical analysis

Statistical analyses were conducted with GraphPad Prism 9.0. Normally distributed data are expressed as the mean ± standard deviation, and non-normally distributed data are expressed as the median (interquartiles range). For normally distributed data, comparisons between two groups were performed by unpaired *t*-tests, and one-way analysis of variance (ANOVA) was used for comparisons among multiple groups. Mann-Whitney *U* tests were used for comparisons between two groups for data that did not conform to a normal distribution, and Kruskal-Wallis (*H*) tests were used for comparisons among multiple groups. For count data, frequencies and percentages were used to describe the differences between groups using the chi-square test or Fisher's exact probability method. Differences were considered statistically significant at *, P<0.05; **, P<0.01; ***, P<0.001; and ****, P<0.0001. The data were derived from at least three independent experiments.

Results

Transcriptomic characterization of atrial tissue from patients with AF

For elucidation of the molecular mechanisms contributing to AF formation, RNA-seq analysis was performed on atrial tissues from patients who underwent valve repair/replacement for AF and SR at the Department of Cardiac Macrovascular Surgery (Figure S5). The analysis revealed that the mean age of the patients with AF was 64.0 years (interquartile range, 51–69 years), with 62.5% being male, whereas the mean age of the patients in the SR group was 61.8 years (interquartile range, 57–76 years), with 80% being male. The ejection fraction (EF%) values were comparable between groups, averaging 63.63%±4.90% in the AF group and 62.8%±2.39% in the SR group. The N-terminal pro b-type natriuretic peptide (NT-proBNP) (pg/mL) (P=0.002), left atrial inner diameter (LAD) (mm) (P=0.01) and Left atrial volume index (LADI) (P<0.001) of the two groups were found to be significantly higher in the AF group than in the SR group. Medical history including hypertension (P>0.99), previous cerebral infarctions (none), diabetes mellitus (none), coronary artery disease (none), smoking history (P>0.99), etc., was notably similar across both groups (Table S1). Based on the COUNT data, 1,870 genes were differentially expressed, 459 of which were upregulated and 1,411 of which were downregulated. The expression patterns of these genes were illustrated by heatmaps and volcano plots (*Figure 1A,1B*). GSEA of the Kyoto Encyclopedia of Genes and Genomes (KEGG) gene set, utilizing the Molecular Signatures Database (MsigDB) database (https://www.gsea-msigdb.org/gsea/msigdb), identified the top 10 KEGG pathways, revealing significant enrichment in pathways such as ubiquitination and the cell cycle in the AF group (*Figure 1C*). Masson's trichrome staining of atrial tissues indicated a greater degree of fibrosis in the patients with AF than in the patients with SR (*Figure 1D*), suggesting the clinical patient model had atrial structural remodeling, which was consistent with the characteristics of ACM.

The expression of STK38L is elevated in the atrial tissues of patients with AF

TGF-β1 is crucial for the development of myocardial fibrosis. Consequently, RNA-seq data (GSE225336) from TGF-β1-stimulated human CFs were chosen for data mining. This dataset included a total of 2,692 DEGs, 593 of which were upregulated and 2,099 of which were downregulated, as depicted in a heatmap (*Figure 2A*). Venn analysis intersected upregulated genes from both GSE225336 dataset and self-assessment dataset, identifying 24 shared genes (*Figure 2B*). Gene Ontology (GO) enrichment analysis of the intersecting genes revealed significant enrichment in biological processes, including growth factor aggregation response and negative regulation of protein

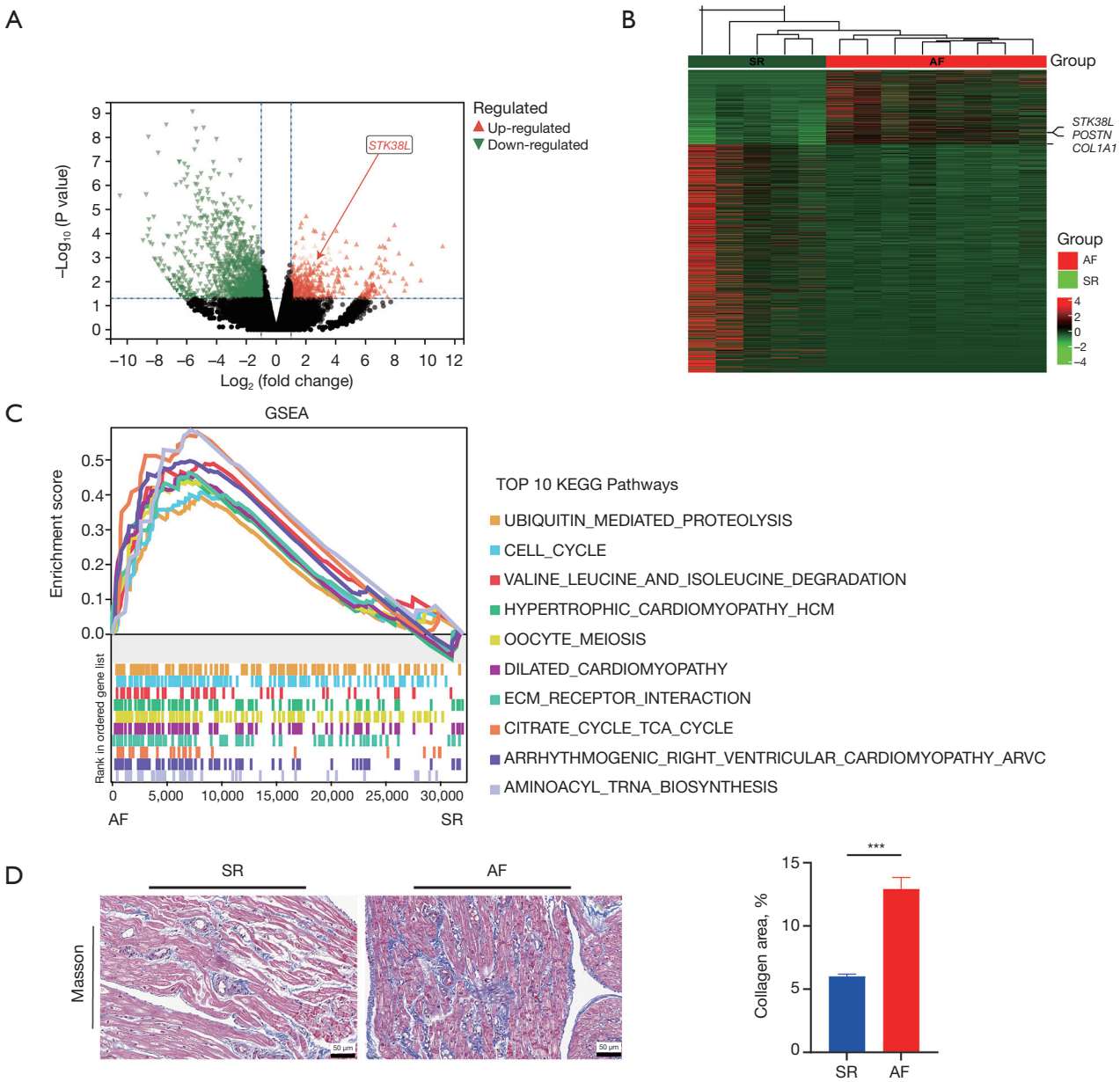

Figure 1 Transcriptomic characterization of atrial tissues in patients with AF. (A) Volcano plot showing the results of the differential gene expression analysis. (B) Heatmap of differential gene expression. (C) GSEA of the top 10 enriched KEGG pathways among the SR and AF groups. (D) Representative images of Masson-trichrome staining of the atrial tissues of each group. Unpaired *t*-test, ***, P<0.001, compared with the SR group. Scale bar =50 μm. STK38L, serine/threonine kinase 38-like; POSTN, periostin; COL1A1, collagen type I alpha 1 chain; AF, atrial fibrillation; SR, sinus rhythm; GSEA, gene set enrichment analysis; KEGG, Kyoto Encyclopedia of Genes and Genomes.

hydrolysis (*Figure 2C*). Alignment corrections utilizing the false discovery rate (FDR) values of intersecting molecules identified *STK38L* as the sole differentially expressed molecule with an FDR <0.05 in the self-assessment data (*Figure 2D*). Validation was performed with another TGF-β1-stimulated human CFs dataset, GSE97358, which revealed elevated *STK38L* expression in the TGF-β1 group through pairwise testing (Figure S6). The protein and mRNA levels of Collagen-I and STK38L were significantly greater in the AF group (*Figure 2E,2F*). The results suggest

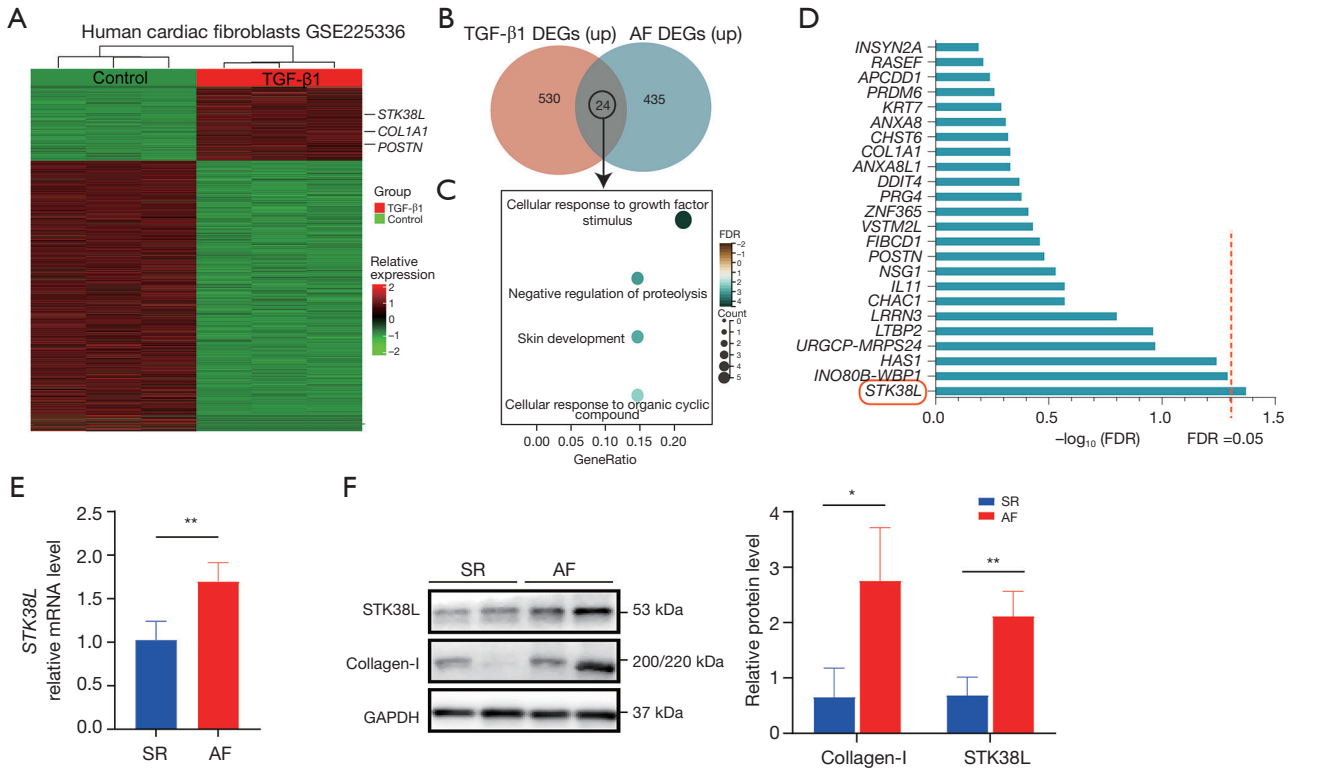

Figure 2 STK38L expression is elevated in the atrial tissues of patients with AF. (A) Heatmap showing DEGs (a total of 2,692 DEGs; 593 were upregulated, and 2,099 were downregulated). The GSE225336 RNA-seq data were from primary human CFs treated with or without human TGF-β1. (B) Venn diagram showing 24 genes in the AF group (435 genes) and the TGF-β1 group (530 genes) according to the GSE225336 RNA-seq data. (C) The 4 most significantly enriched GO terms of the intersecting genes. (D) The intersecting genes are presented in descending order of $-\log_{10}$ (FDR). (E) The *STK38L* mRNA level in the SR and AF groups was normalized to that of *GAPDH* (n=4). (F) The protein level of STK38L, Collagen-1 in the SR and AF groups was normalized to that of GAPDH (n=4); Unpaired *t*-test, *, P<0.05; **, P<0.01. STK38L, serine/threonine kinase 38-like; POSTN, periostin; COL1A1, collagen type I alpha 1 chain; TGF-β1, transforming growth factor β1; DEGs, differentially expressed genes; AF, atrial fibrillation; FDR, false discovery rate; SR, sinus rhythm; RNA-seq, RNA sequencing; CFs, cardiac fibroblasts; GO, Gene Ontology.

that STK38L is likely involved in AF-related and TGF-β1-related myocardial fibrosis.

STK38L expression is elevated in mouse primary CFs stimulated with TGF-β1

To investigate the potential involvement of *STK38L* in TGF-β1-induced cardiac fibrosis, we analyzed RNA-seq data from the GSE132143 dataset of mouse CFs stimulated with TGF-β1. A TGF-β1-stimulated mouse primary CFs model was established for experimental validation (Figure S3). Significant increases in STK38L, periostin (POSTN), and Collagen-I expression in the TGF-β1 group were demonstrated by both polymerase chain reaction (PCR) and Western blotting (*Figure 3A*,*3B*). Subsequently, to understand the enrichment of *STK38L* in cardiac tissue, single-cell RNA-seq data from a transverse aortic constriction (TAC)-induced mouse model in the GSE120064 dataset were analyzed, and fibroblasts were screened by cell sorting (Figure S7A). Analysis of gene expression density revealed an increase in *STK38L* expression within the activated region of CFs, characterized by high expression of *POSTN* and collagen type I alpha 1 chain (*COL1A1*) (Figure S7B). This finding again suggests that STK38L may play an important role in CFs.

Si-STK38L inhibits CF activation and proliferation

An experimental verification was conducted to assess the impact of STK38L on the activation and proliferation of

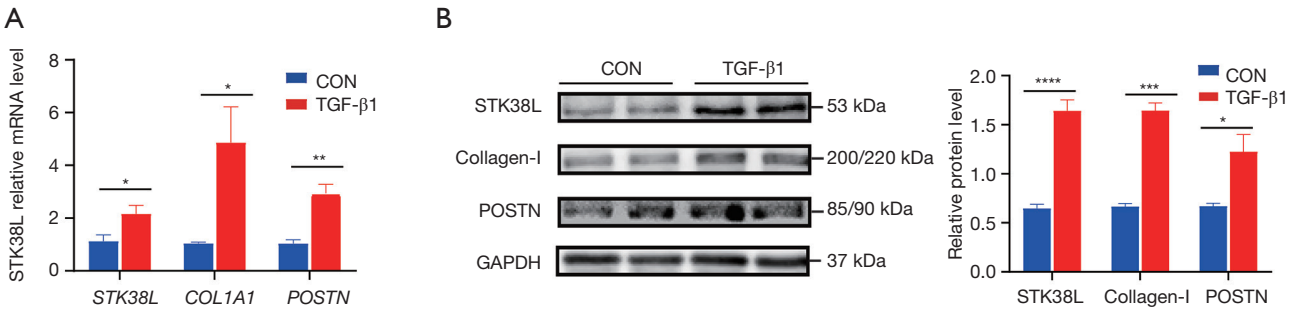

Figure 3 STK38L expression is elevated in mouse primary CFs stimulated with TGF-β1. (A) *STK38L*, *COL1A1* and *POSTN* mRNA expression normalized to *GAPDH* mRNA expression in the CON- and TGF-β1-treated CFs (n=4). (B) Protein levels of STK38L, Collagen-I, and POSTN were normalized to those of GAPDH in the CON- and TGF-β1-treated CFs (n=4). *, P<0.05; **, P<0.01; ***, P<0.001; ****, P<0.0001. STK38L, serine/threonine kinase 38-like; COL1A1, collagen type I alpha 1 chain; POSTN, periostin; CON, control; TGF-β1, transforming growth factor β1; CFs, cardiac fibroblasts.

mouse CFs. Mouse primary CFs were initially stimulated with TGF-β1 for 24 h, followed by transfection with STK38L-siRNA (Figure S4). We used various siRNA tools capable of inhibiting gene expression and found that the mRNA expression of *STK38L* decreased (*Figure 4A*). After TGF-β1 stimulation, si-STK38L inhibited the protein level of STK38L, POSTN, and Collagen-I in CFs (*Figure 4B*). Furthermore, STK38L inhibition suppressed CFs migration and proliferation, as demonstrated by the scratch and Cell Counting Kit-8 (CCK-8) assays (*Figure 4C,4D*). These results indicate that STK38L is crucial for the activation and proliferation of CFs. SKT38L inhibition leads to the suppression of these processes.

STK38L expression is significantly elevated in the ISO-induced mouse model of myocardial fibrosis

Finally, this study explored the changes in *STK38L* expression in the cardiac tissues of mice subcutaneously stimulated with ISO (ISO mice). The levels of *STK38L* in the cardiac tissues of the ISO mice were first analyzed using the GSE82294 dataset, where a significant increase in *STK38L* mRNA expression in the ISO group was observed, along with a positive correlation with *COL1A1* expression (Spearman cor =0.3606, Figure S8). Subsequently, ISO mice were generated, and ventricular tissues were obtained for PCR validation. Consistent with previous findings, significant elevations in the expression of *STK38L*, *POSTN*, and *COL1A1* were observed in the heart tissues of the ISO group (*Figure 5A*). Furthermore, a substantial increase in the region of myocardial fibrosis was observed in the ISO mice (*Figure 5B*). These results suggest that STK38L may play a role in the development of ISO-induced myocardial fibrosis in mice

Discussion

AF is the pathogenic factor and clinical manifestation of ACM, similar to the two sides of a coin, which are mutually causative and inseparable. Patients with AF-related ACM often exhibit atrial dilatation and elevated NT-proBNP, which are often closely related to clinical events such as stroke and poor radiofrequency prognosis (6). Therefore, exploring the pathogenic mechanism in such patients is highly important. The clinical data analysis of this study showed that the left atrial index (LADI) of the patients in the disease group (AF) was significantly greater than that of the patients in the control group (SR) (P<0.001), accompanied by increased NT-pro-BNP levels in the blood (P=0.002) (Table S1), and Masson staining revealed obvious fibrosis of the atrial tissue (P<0.001) (*Figure 1D*). The above data are consistent with the clinical characteristics of AF-related ACM (17,18) and have clinical research value. Based on the above typical clinical cases, we studied the underlying pathogenic mechanism and discovered through bioinformatics analysis that STK38L may be involved in myocardial fibrosis. We used human clinical samples, mouse models, and cell models to demonstrate that STK38L expression is increased during myocardial fibrosis. In this case, STK38L reduction may be beneficial for cardiac structural remodeling.

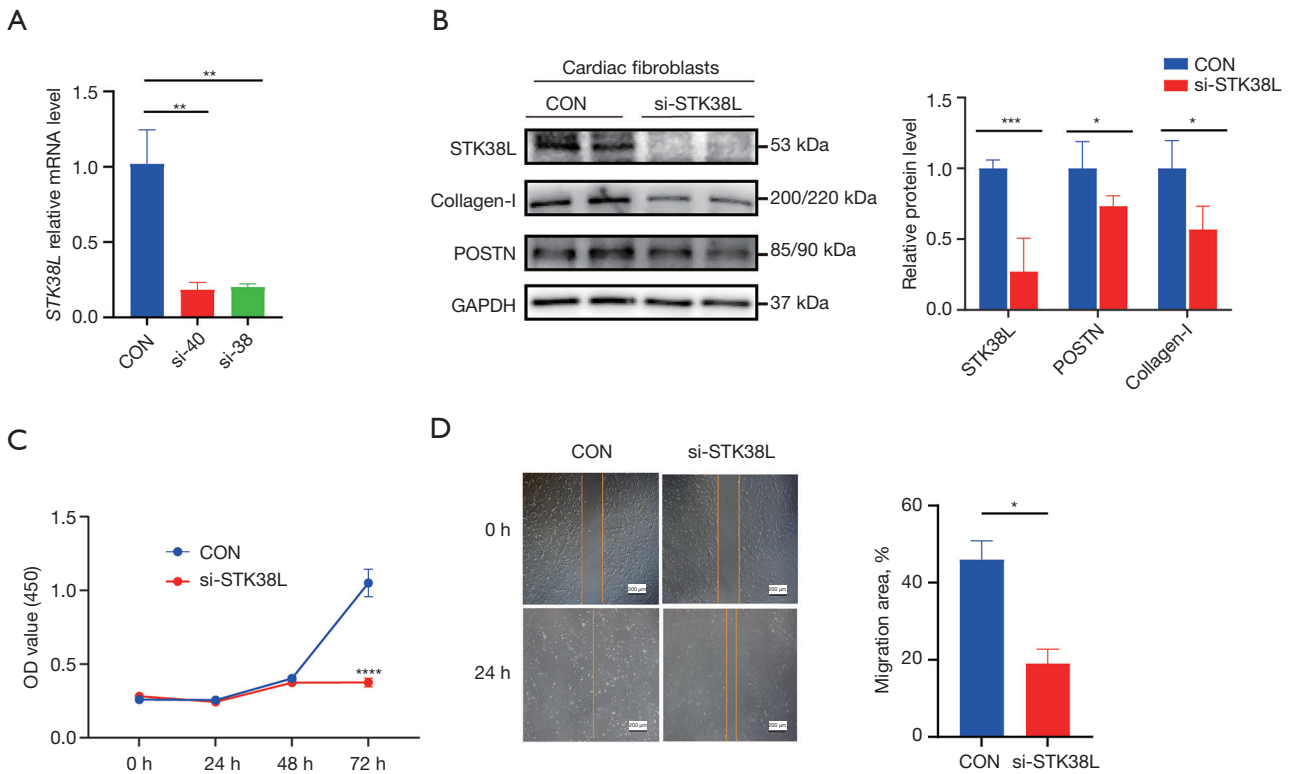

Figure 4 Si-STK38L inhibits CFs activation and proliferation. (A) Validation of the knockdown efficacy of si-*STK38L* (si-40 and si-38) in TGF-β1-stimulated mouse CFs (n=4). (B) Protein expression of STK38L, Collagen-I, and POSTN in the CON and si-STK38L-treated CFs (n=4). (C) Cell proliferation after transfection with si-STK38L was assessed by the CCK-8 assay (n=6). (D) A cell scratch assay was used to assess the proliferative capacity of cells after si-STK38L transfection at 0 and 24 h (n=3). Scale bar =200 μm. Unpaired *t*-test, *, P<0.05; **, P<0.01; ***, P<0.001; ****, P<0.0001. CON, control group; si, siRNA group; STK38L, serine/threonine kinase 38-like; Collagen-I, collagen type I alpha 1 chain; POSTN, periostin; OD, optical density; CFs, cardiac fibroblasts; TGF-β1, transforming growth factor β1; CCK-8, Cell Counting Kit-8.

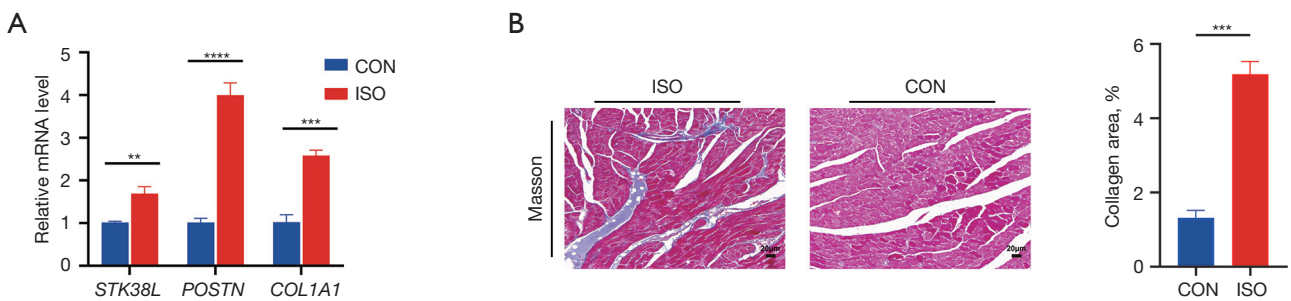

Figure 5 STK38L expression is significantly elevated in an ISO-induced mouse model of myocardial fibrosis. (A) mRNA levels of *STK38L*, *COL1A1*, and *POSTN* were normalized to those of *GAPDH* in the CON and ISO groups (n=3). (B) Typical Masson's trichrome stain images of the CON and ISO groups (n=3). Scale bar =20 μm. Unpaired *t*-test, **, P<0.01; ***, P<0.001; ****, P<0.0001. STK38L, serine/threonine kinase 38-like; COL1A1, collagen type I alpha 1 chain; POSTN, periostin; CON, control; ISO, isoprenaline.

To analyze the mechanism of disease development, we collected atrial tissues from two groups of patients for RNA-seq analysis and identified 1,870 DEGs. KEGG analysis revealed that the top 10 KEGG pathways included ubiquitination, cell cycle, cardiomyopathy, and ECM receptor interaction pathways. Among these pathways, the ECM interaction pathway is closely related to myocardial fibrosis, is mainly promoted by transmembrane molecules (such as integrins) and is closely related to fibroblast migration and TGF-β1 activation (19). TGF-β1 is one of the best-known pleiotropic fibrogenic growth factors, and promotes the synthesis of ECM proteins (20). Therefore, we selected RNA-seq data related to human primary CFs stimulated with TGF-β1 from the GEO dataset GSE225336 and self-measured AF RNA-seq data. Twenty-four common genes were identified in the upregulated gene sets of both groups. GO functional analysis revealed that these genes were mainly enriched in the response of cells to growth factor aggregation, suggesting that the common genes may be related to processes such as cell growth, proliferation and migration. These genes include myocardial fibrosis markers such as *COL1A1* (21), *POSTN* (22), and *LTBP2* (23), indicating that the two groups of test samples had a clear trend of fibrosis. However, only *STK38L* significantly differed (FDR <0.05). For repeated verification, we performed paired tests on the GSE97358 dataset, and the results showed that *STK38L* was also elevated in human primary CFs after 16 h of TGF-β1 stimulation (Figure S6). Subsequently, PCR and Western blotting were performed on atrial tissues of patients, and the results were consistent (*Figure 2E,2F*). Therefore, it is hypothesized that the high expression of STK38L may be associated with the progression of cardiac fibrosis.

Given that STK38L is highly conserved in different species of eukaryotes (24) and considering medical ethical restrictions of human, this study investigated its expression using readily available mouse models (both animal and cellular models). Since activated fibroblasts are the primary effector cells in cardiac fibrosis (25), gaining a better understanding of the CFs responsible for collagen production will be key to finding methods to inhibit excessive ECM (26). First, we analyzed the GSE132143 data. The heatmap shows that after primary CFs of adult mouse were stimulated with TGF-β1, the mRNA levels of *POSTN* and *STK38L* increased (Figure S9). POSTN is downstream of the TGF-β1 pathway and elevated expression levels are closely related to myocardial fibrosis. Subsequently, we conducted experimental validation via PCR and Western blotting in TGF-β1-stimulates primary CFs of neonatal mice, obtaining reproducible results (*Figure 3A,3B*). Secondly, we analyzed the single-cell RNA-seq data (GSE120064) from the TAC mouse models to investigate the potential cellular distribution of STK38L in the hearts with myocardial fibrosis. TAC-induced mice are the most commonly used animal surgical model for studying pressure overload-induced left ventricular hypertrophy (27), which mainly characterized by myocardial fibrosis-induced remodeling (28). Through these data, we initially identified cardiomyocytes, CFs, macrophages, and cardiac endothelial cells through cell classification (Figure S7A). Through gene expression density calculations, we found that not only did myocardial fibrosis indicators such as *POSTN* and *COL1A1* increase in the CFs of the TAC group but also *STK38L* expression was primarily enriched in these cells (Figure S7B), suggesting that STK38L may play a role in activated fibroblasts. Thirdly, we detected whether STK38L has a regulatory function on CFs. Using STK38L-siRNA to downregulate STK38L expression in CFs stimulated with TGF-β1 decreased the expression levels of POSTN and Collagen I (*Figure 4A,4B*), proving that STK38L downregulation can inhibit ECM production. CCK-8 and scratch assays showed that downregulation of STK38L inhibited CFs proliferation and migration (*Figure 4C,4D*). Based on the above conclusions, inhibiting STK38L expression may inhibit the progression of myocardial fibrosis. Similarly, Zhou *et al.* reported that methyltransferase-like 3 (METTL3) promotes cardiac fibrosis by increasing CFs proliferation and glycolysis (29).

Most of the heart tissue belongs to the ventricle. In 2010, Thin Thin Aye analyzed more than 130,000 MS/MS spectra and found that STK38L is also present in large quantities in the left ventricle of the human heart (30). Therefore, it is speculated that abnormal expression of STK38L may cause ventricular-related diseases. In a 2015 analysis of human Affymetrix microarray data, it was found that *STK38L* expression in the hearts of patients with heart failure was significantly higher compared to the control group without heart failure (31). Based on the above results, we chose to construct a mouse model of myocardial fibrosis via continuous subcutaneous injection of ISO in adult mice and selected ventricular tissue for *in vivo* verification. ISO can promote myocardial cell hypertrophy and subsequently cause pathological myocardial hypertrophy. Long-term treatment eventually causes myocardial fibrosis and heart failure (32). In this study, Masson's trichrome staining

revealed that the ventricular tissue of the mice in the ISO group exhibited obvious fibrotic phenotypes, and PCR confirmed that the *STK38L* mRNA level was increased in the ISO group, which was the same trend as in heart failure patients.

The limitations of the current study are as follows: (I) the differences in the protein abundance of STK38L in different parts of the heart can be further confirmed through animal models or clinical samples. In the future, tissue-specific knockout mouse models can be designed based on the abundance in different tissues to accurately determine the role of STK38L in specific cardiac tissue diseases, such as AF. (II) This study focused mainly on the role of STK38L in myocardial fibrosis, and the pathogenesis of myocardial fibrosis is complex and may involve the regulation of multiple molecular pathways. Therefore, future studies should combine STK38L with other potential targets, and even include different cell types, such as cardiomyocytes and cardiac immune cells, to further elucidate the pathogenesis of myocardial fibrosis. (III) This study observed a phenomenon, but the specific molecular mechanism remains unexplored. Based on tumor cell studies, STK38L can regulate the phosphorylation of ser146 of P21 protein, impacting the cell cycle progression of HeLa cells (33). While this mechanism could explain STK38L's effect on cell proliferation, its applicability in CFs requires further experimental verification.

Conclusions

STK38L is a kinase with multiple functional effects. In our study, this molecule was found to act mainly on CFs and to be closely related to the progression of myocardial fibrosis. Inhibiting STK38L expression may hinder ECM formation and CFs proliferation and migration, thereby delaying myocardial fibrosis. As we did not fully elucidate the mechanism of action of STK38L in heart disease, future studies should clarify its specific functions and potential therapeutic applications and develop personalized medical strategies and inhibitors for STK38L based on the genetic background, clinical characteristics and molecular phenotype of individual patients to achieve more precise therapeutic effects.

Acknowledgments

We would like to thank Lea Moore and AJE Support for their help in polishing our paper.

Funding: This study was supported by Anhui Medical University School Research Clinical Science Fund Project (No. 2023xkj166).

Footnote

Reporting Checklist: The authors have completed the ARRIVE reporting checklist. Available at https://cdt.amegroups.com/article/view/10.21037/cdt-24-164/rc

Data Sharing Statement: Available at https://cdt.amegroups.com/article/view/10.21037/cdt-24-164/dss

Peer Review File: Available at https://cdt.amegroups.com/article/view/10.21037/cdt-24-164/prf

Conflicts of Interest: All authors have completed the ICMJE uniform disclosure form (available at https://cdt.amegroups.com/article/view/10.21037/cdt-24-164/coif). The authors have no conflicts of interest to declare.

Ethical Statement: The authors are accountable for all aspects of the work in ensuring that questions related to the accuracy or integrity of any part of the work are appropriately investigated and resolved. The study was conducted in accordance with the Declaration of Helsinki (as revised in 2013). The study was approved by the ethics committee of The Second Affiliated Hospital of Anhui Medical University (No. YX2022-099) and informed consent was taken from all the patients. Animal experiments were performed under a project license (No. 20170296) granted by the Institutional Animal Care and Use Committee at Anhui Medical University, in compliance with institutional guidelines for the care and use of animals.

References

1. Kurose H. Cardiac Fibrosis and Fibroblasts. Cells

2021;10:1716.
2. Maruyama K, Imanaka-Yoshida K. The Pathogenesis of Cardiac Fibrosis: A Review of Recent Progress. Int J Mol Sci 2022;23:2617.
3. Bildyug N. Extracellular Matrix in Regulation of Contractile System in Cardiomyocytes. Int J Mol Sci 2019;20:5054.
4. Goette A, Kalman JM, Aguinaga L, et al. EHRA/HRS/APHRS/SOLAECE expert consensus on atrial cardiomyopathies: definition, characterization, and clinical implication. Europace 2016;18:1455-90.
5. Hermans BJM, Weberndörfer V, Bijvoet GP, et al. New concepts in atrial fibrillation pathophysiology. Herzschrittmacherther Elektrophysiol 2022;33:362-6.
6. Baman JR, Cox JL, McCarthy PM, et al. Atrial fibrillation and atrial cardiomyopathies. J Cardiovasc Electrophysiol 2021;32:2845-53.
7. D'Alessandro E, Winters J, van Nieuwenhoven FA, et al. The Complex Relation between Atrial Cardiomyopathy and Thrombogenesis. Cells 2022;11:2963.
8. Grant TJ, Mehta AK, Gupta A, et al. STK38L kinase ablation promotes loss of cell viability in a subset of KRAS-dependent pancreatic cancer cell lines. Oncotarget 2017;8:78556-72.
9. Kleemann M, Schneider H, Unger K, et al. Induction of apoptosis in ovarian cancer cells by miR-493-3p directly targeting AKT2, STK38L, HMGA2, ETS1 and E2F5. Cell Mol Life Sci 2019;76:539-59.
10. Wang S, Chu F, Xia R, et al. LPA maintains innate antiviral immunity in a pro-active state via STK38L-mediated IRF3 Ser303 phosphorylation. Cell Rep 2022;41:111661.
11. Hergovich A. The Roles of NDR Protein Kinases in Hippo Signalling. Genes (Basel) 2016;7:21.
12. Demiray YE, Rehberg K, Kliche S, et al. Ndr2 Kinase Controls Neurite Outgrowth and Dendritic Branching Through α(1) Integrin Expression. Front Mol Neurosci 2018;11:66.
13. Smith N, Reznik E, Bisikirska B, et al. Kinases Controlling Stability of the Oncogenic MYCN Protein. ACS Med Chem Lett 2023;14:1664-72.
14. Ding JF, Sun H, Song K, et al. IGFBP3 epigenetic promotion induced by METTL3 boosts cardiac fibroblast activation and fibrosis. Eur J Pharmacol 2023;942:175494.
15. Qian H, Lu Z, Hao C, et al. TRIM44 aggravates cardiac fibrosis after myocardial infarction via TAK1 stabilization. Cell Signal 2023;109:110744.
16. Wang Q, Liang S, Qian J, et al. OTUD1 promotes isoprenaline- and myocardial infarction-induced heart failure by targeting PDE5A in cardiomyocytes. Biochim Biophys Acta Mol Basis Dis 2024;1870:167018.
17. Chen J, Gao F, Liu W. Atrial cardiopathy in embolic stroke of undetermined source. Brain Behav 2021;11:e02160.
18. Rossi VA, Krizanovic-Grgic I, Steffel J, et al. Predictors of left atrial fibrosis in patients with atrial fibrillation referred for catheter ablation. Cardiol J 2022;29:413-22.
19. Chen C, Li R, Ross RS, et al. Integrins and integrin-related proteins in cardiac fibrosis. J Mol Cell Cardiol 2016;93:162-74.
20. Jolly AJ, Lu S, Dubner AM, et al. Redistribution of the chromatin remodeler Brg1 directs smooth muscle-derived adventitial progenitor-to-myofibroblast differentiation and vascular fibrosis. JCI Insight 2023;8:e164862.
21. Patrawalla NY, Kajave NS, Albanna MZ, et al. Collagen and Beyond: A Comprehensive Comparison of Human ECM Properties Derived from Various Tissue Sources for Regenerative Medicine Applications. J Funct Biomater 2023;14:363.
22. Nagalingam RS, Chattopadhyaya S, Al-Hattab DS, et al. Scleraxis and fibrosis in the pressure-overloaded heart. Eur Heart J 2022;43:4739-50.
23. Pang XF, Lin X, Du JJ, et al. LTBP2 knockdown by siRNA reverses myocardial oxidative stress injury, fibrosis and remodelling during dilated cardiomyopathy. Acta Physiol (Oxf) 2020;228:e13377.
24. Sharif AAD, Hergovich A. The NDR/LATS protein kinases in immunology and cancer biology. Semin Cancer Biol 2018;48:104-14.
25. Frangogiannis NG. Cardiac fibrosis. Cardiovasc Res 2021;117:1450-88.
26. Venugopal H, Hanna A, Humeres C, et al. Properties and Functions of Fibroblasts and Myofibroblasts in Myocardial Infarction. Cells 2022;11:1386.
27. deAlmeida AC, van Oort RJ, Wehrens XH. Transverse aortic constriction in mice. J Vis Exp 2010;1729.
28. Chen X, Li X, Wu X, et al. Integrin beta-like 1 mediates fibroblast-cardiomyocyte crosstalk to promote cardiac fibrosis and hypertrophy. Cardiovasc Res 2023;119:1928-41.
29. Zhou Y, Song K, Tu B, et al. METTL3 boosts glycolysis and cardiac fibroblast proliferation by increasing AR methylation. Int J Biol Macromol 2022;223:899-915.
30. Aye TT, Scholten A, Taouatas N, et al. Proteome-wide protein concentrations in the human heart. Mol Biosyst 2010;6:1917-27.
31. Fuller SJ, Osborne SA, Leonard SJ, et al. Cardiac protein

kinases: the cardiomyocyte kinome and differential kinase expression in human failing hearts. Cardiovasc Res 2015;108:87-98.
32. Karam S, Margaria JP, Bourcier A, et al. Cardiac Overexpression of PDE4B Blunts β-Adrenergic Response and Maladaptive Remodeling in Heart Failure. Circulation 2020;142:161-74.
33. Cornils H, Kohler RS, Hergovich A, et al. Human NDR kinases control G(1)/S cell cycle transition by directly regulating p21 stability. Mol Cell Biol 2011;31:1382-95.

Cite this article as: Zhang Y, Zhang R, Wang X, Fang S, Wang B. Role of STK38L in atrial fibrillation-associated myocardial fibrosis: findings from RNA-seq analysis. Cardiovasc Diagn Ther 2024;14(5):798-809. doi: 10.21037/cdt-24-164